

# Combined Neodymium–Ytterbium-Doped ASE Fiber-Optic Source for Optical Coherence Tomography Applications

I. Trifanov, P. Caldas, L. Neagu, R. Romero, M. O. Berendt, J. A. R. Salcedo, A. Gh. Podoleanu, and António B. Lobo Ribeiro

**Abstract**—Optical coherence tomography (OCT) imaging at the 1060-nm region proved to be a successful alternative in ophthalmology not only for resolving intraretinal layers, but also for enabling sufficient penetration to monitor the subretinal vasculature in the choroid when compared to most commonly used OCT imaging systems at the 800-nm region. To encourage further clinical research at this particular wavelength, we have developed a compact fiber-optic source based on amplified spontaneous emission (ASE) centered at  $\sim 1060$  nm with  $\sim 70$ -nm spectral bandwidth at full-width at half-maximum and output power  $>20$  mW. Our approach is based on a combination of slightly shifted ASE emission spectra from a combination of Neodymium- and Ytterbium-doped fibers. Spectral shaping and power optimization have been achieved using in-fiber filtering schemes. We have tested the performance of the source in an OCT system optimized for this wavelength.

**Index Terms**—ASE optical source, broadband fiber source, optical coherence tomography.

## I. INTRODUCTION

THE most used wavelength band for optical coherence tomography (OCT) of the retina has been 800 nm, justified by low absorption in the vitreous and the availability of low cost and high power superluminescent diode (SLD). Interest has been manifest recently in longer wavelengths, given the increased penetration in the deeper layers in the retina, such as into the choroid, due to decrease of scattering by increasing the wavelength. The 1020–1080 nm region of the near-infrared

spectrum emerged as an attractive option for imaging the retina due to a relative minimum of the water absorption coefficient at 1060 nm. The potential for retina imaging in the 1020–1080 nm region has already been demonstrated *ex vivo* and *in vivo* using A-scan-based time-domain OCT [1], [2] and *in vivo* using swept source OCT [3]. There is however a fundamental limitation to the highest axial resolution achievable determined by the reduced full-width-half-maximum (FWHM) of the water absorption window, that is centered at  $\sim 1060$  nm which limits the axial resolution in human retina to  $\sim 3.6$   $\mu\text{m}$ . So far, axial resolutions of up to 5.7  $\mu\text{m}$  has been achieved *in-vivo* with a modified SLD source integrated into a spectral domain OCT (SD-OCT) system. The reported value explicitly takes into account the spectral absorption of transmitted radiation through 25 mm of water [4]. Broadband sources such as SLDs [5] and fiber ASE sources [6] may comply with the bandwidth requirement for ultrahigh resolution, but they are mostly 10 or 20 nm below the centre of the water absorption optical window. This severely impacts the bandwidth and optical power transmitted to the retinal tissue. Therefore, other directions have been considered, such as development of rare-earth doped fibers with broadband amplified stimulated emission (ASE) around 1060 nm [7]. One possibility is that of ASE sources based on Neodymium (Nd) doped fiber (centered at 1060 nm), except for their relatively narrow optical bandwidth of  $<17$  nm. Another candidate whose emission center is around 1040 nm is Ytterbium (Yb), which can exhibit a FWHM of  $\sim 30$  nm. Reshaping using either free-space or all-fiber optic components can improve optical bandwidth of such sources and shift their central wavelength significantly (75 nm centered at 1060 nm reported in [8]). An all-fiber optical design is preferable for higher efficiency and stability.

Our approach in designing an ASE source is primarily based on meeting the requirements imposed by the water absorption window. The source architecture is build on a careful combination of tailored superfluorescence from Ytterbium (Yb) doped and Neodymium (Nd) doped silica fibers pumped by commercial diode lasers. Similar combinations have been reported previously, integrated in different architectures, their primarily goal being to extend the Yb emission towards longer wavelength range using bulk optical arrangement for tailoring the spectrum [9]. Such an approach gives a high flexibility over the output shape of the spectrum, while there are disadvantages related to very high sensitivity to small reflections of the output into the pump source and significant loss in power due to double-passing

Manuscript received May 10, 2010; revised October 19, 2010; accepted October 24, 2010. Date of publication October 28, 2010; date of current version December 22, 2010. This work was supported in part by the European project HIRESONI (Marie Curie EC MEST-CT-2005-020353).

I. Trifanov, L. Neagu, R. Romero, M. O. Berendt, and J. A. R. Salcedo are with Multiwave Photonics S.A., 4470-605 Moreira da Maia, Portugal (e-mail: itrifanov@multiwavephotonics.com; lneagu@multiwavephotonics.com; rromero@multiwavephotonics.com; moberendt@multiwavephotonics.com; jsalcedo@multiwavephotonics.com).

P. Caldas is with UOSE, INESC-Porto, 4150-179 Porto, Portugal (e-mail: pcaldas@inescporto.pt).

A. G. Podoleanu is with Applied Optics Group, School of Physical Sciences, University of Kent, Canterbury, Kent CT2 7NR, U.K. (e-mail: A.G.H.Podoleanu@ukc.ac.uk).

A. B. Lobo Ribeiro is with Faculty of Health Sciences, University Fernando Pessoa, 4200-150 Porto, Portugal (e-mail: alobo@ufp.edu.pt).

Color versions of one or more of the figures in this letter are available online at <http://ieeexplore.ieee.org>.

Digital Object Identifier 10.1109/LPT.2010.2090039

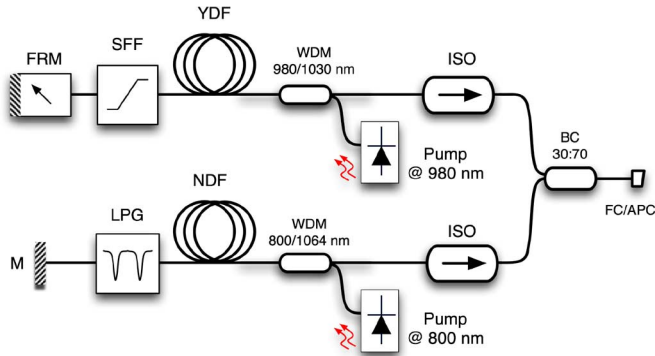


Fig. 1. Experimental setup of the combined Neodymium–Ytterbium-doped ASE fiber source.

through the filter, especially, if high pump powers are not available. With significant spectral reshaping based on a compact in-fiber optical solution, a source was assembled that emits at a central wavelength of 1060 nm and exhibits a FWHM exceeding 70 nm and 20 mW output power. The approach can be further optimized in terms of output power and flatter spectrum with improved FWHM value.

## II. METHOD AND RESULTS

One challenge in designing a fiber based broadband source is to extract large ASE powers while avoiding laser oscillations. Lasing can occur due to optical feedback from component reflections and/or from Rayleigh backscattering. Fiber optical isolators are required even if low back-reflections from all components and splices are ensured. Larger ASE power densities can be reached before the onset of lasing when a Faraday rotator mirror (FRM) is used [10]. Another important issue to consider is the degree of population inversion which influences the spectral shape through interplay between emission and absorption spectra for Yb-doped fiber in the 1060 nm spectral range.

Fig. 1, illustrates the configuration of our combined ASE source, with double backward pumping configuration and filtered forward ASE seeding, with special spectral flattening filter (SFF) [11]. A 5 m length of Yb-doped fiber (YDF), is pumped at 975.5 nm (pump power: 165 mW) through a thin-film WDM 980/1030 nm fiber coupler, combined through a 30:70 splitting ratio broadband output coupler (BC), with a  $\sim 5$  m length of Nd-doped fiber (NDF) pumped at 808 nm (pump power: 100 mW) through a thin-film WDM 800/1064 nm fiber coupler. An in-house long-period fiber grating (LPG) with appropriate spectral characteristics was fabricated in HI1060 fiber by electric arc-discharge method [12], to induce an excess loss at the dominant band of the original Nd double-pass backward ASE spectrum. No spurious lasing was observed at the maximum 808 nm pump power with a gold mirror (M) as optical feedback, and thus no need for a FRM at this port. Fig. 2 shows the output spectrum of the combined Nd–Yb-doped ASE fiber source. This fiber source delivers more than 20 mW nonpolarized output power in single transverse mode, centered at 1058 nm wavelength with a FWHM spectral bandwidth exceeding 70 nm. We have measured the source autocorrelation function (shown in Fig. 3) using a Michelson interferometer wavelength meter (HP 8612B modified in-house). This shows: a) that an axial resolution of  $7 \mu\text{m}$

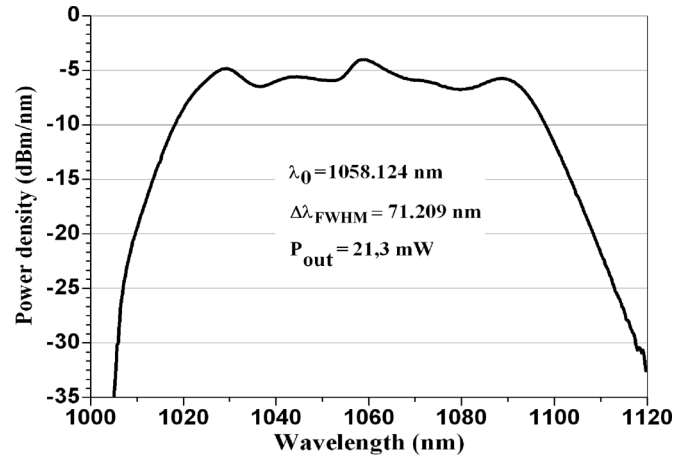


Fig. 2. Output spectrum of the combined ASE fiber source.

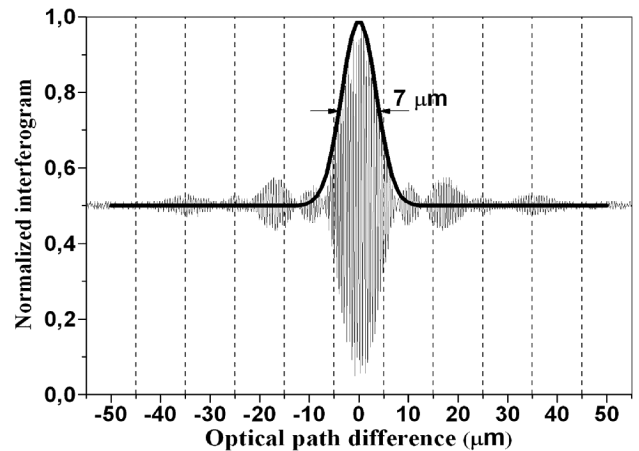


Fig. 3. Normalized interferogram of the combined ASE source.

is achievable in air and  $\sim 5 \mu\text{m}$  in tissue assuming a refractive index of 1.4 and using the values for the bandwidth and central wavelength of Fig. 2); b) the profile exhibits secondary peaks or side lobes, with amplitudes close to 10% of the main peak magnitude, due to the non-Gaussian profile of the spectrum. This can cause severe coherent artifacts in the OCT image. Postprocessing of the coherence function has been employed to minimize such unwanted effects, which lead to a reduction of the secondary lobes to less than 5%.

## III. APPLICATION ON OCT IMAGING

The source has been properly packaged and tested in a simplified time-domain OCT system optimized for this wavelength range [13]. The system is capable of acquiring *en-face* as well as cross-sectional OCT images. A confocal channel was also implemented by diverting a small part of the signal returning from the sample into a Silicon avalanche photodetector with enhanced sensitivity at longer wavelengths. The main advantage of the OCT over the confocal microscopy is that OCT achieves very high axial image resolution, independent of the focusing condition, while the lateral resolution is practically the same in both imaging channels and is defined by the focal spot size [14]. In all subsequent retinal OCT images, the axial resolution is given by the coherence length of the source modified by the transfer function of the OCT system. The measured value is  $15 \mu\text{m}$  in tissue, slightly worse than the theoretical value,

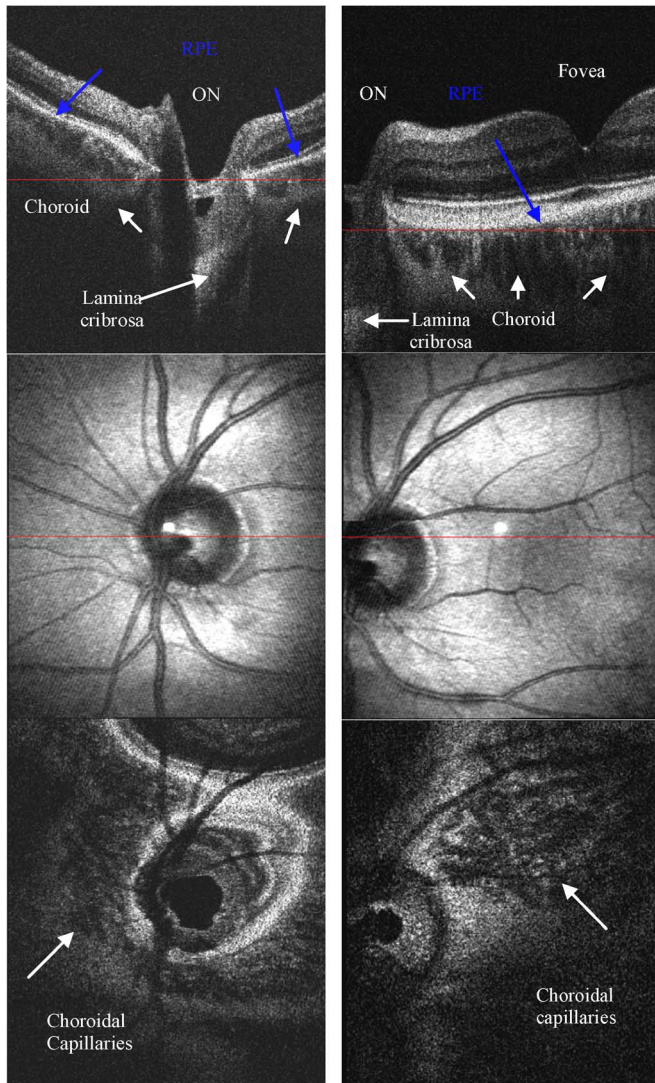


Fig. 4. *In vivo* images of the retina of a volunteer. Top: Cross-sectional OCT images; lateral size: 6 mm; axial size: 2.5 mm measured in air; centered on the optic nerve (ON) (left) and displaying the fovea and parts of the optic nerve (right). Middle and bottom: Pairs of simultaneously acquired confocal (middle row)/*en-face* OCT (bottom row); the lateral image size is 6 mm  $\times$  6 mm. Red line over the confocal image (middle) shows where the cross section OCT image is collected from. The red line over the cross section image shows the depth where the *en-face* OCT image in the bottom is collected from.

due to some unbalanced dispersion and polarization in the OCT system. The lateral resolution is limited by the beam diameter and the optics of the eye to about  $\sim 15 \mu\text{m}$ . The power incident on the cornea was 3 mW, below the maximum permissible exposure limits recommended by the American Standards National Institute (ANSI).

Two cross-sectional *in-vivo* OCT images of the human eye fundus at 1060 nm are shown in the top row of Fig. 4, displaying well-defined retinal layers [15], as well as, superior penetration into the choroid, below the retinal pigment epithelium (RPE). Sufficient details are seen at this depth, where at 800 nm, penetration in the retina does not reach the level of depth where the lamina is. The next two rows illustrate pairs of confocal (middle) and *en-face* OCT (bottom) images, where the OCT image was acquired at different depth positions, indicated by the red line in each corresponding cross-sectional OCT image. During the

switch from the *en-face* regime to the cross sectioning regime, the eye may have moved slightly laterally.

Both retinal and choroidal vasculature are visible in the confocal images superimposed due to larger than 1 mm depth of focus. Depth resolved images are provided by the *en-face* OCT (bottom row) showing choroidal capillaries in detail.

#### IV. CONCLUSION

To summarize, we have developed and characterized a broadband ASE source centered at 1060 nm wavelength region, based on a combination of Nd/Yb-doped fibers, for OCT imaging of human retina. Higher power, broader ASE bandwidth and smoother spectrum are achievable by increasing the pump power and/or designing a better filter.

#### REFERENCES

- [1] A. Unterhuber, B. Povozay, B. Hermann, H. Sattmann, A. Chavez-Pirson, and W. Drexler, "In vivo retinal optical coherence tomography at 1040 nm—Enhanced penetration into the choroid," *Opt. Express*, vol. 13, pp. 3252–3258, 2005.
- [2] B. Povozay, K. Bizheva, B. Hermann, A. Unterhuber, H. Sattmann, A. F. Fercher, W. Drexler, C. Schubert, P. K. Ahnelt, M. Mei, R. Holzwarth, W. J. Wadsworth, J. C. Knight, and P. S. J. Russel, "Enhanced visualization of choroidal vessels using ultrahigh resolution ophthalmic OCT at 1050 nm," *Opt. Express*, vol. 11, pp. 1980–1986, 2003.
- [3] E. C. Lee, J. F. de Boer, M. Mujat, H. Lim, and S. H. Yun, "In vivo optical frequency domain imaging of human retina and choroid," *Opt. Express*, vol. 14, pp. 4403–4411, 2006.
- [4] S. Hariri, A. A. Moayed, A. Dracopoulos, C. Hyun, S. Boyd, and K. Bizheva, "Limiting factors to the OCT axial resolution for in-vivo imaging of human and rodent retina in the 1060 nm wavelength range," *Opt. Express*, vol. 17, pp. 24304–24316, 2009.
- [5] Superlum Inc. Ireland, 2010.
- [6] A. Chavez-Pirson, S. Jiang, and W. Tian, "1- $\mu\text{m}$  Phosphate-Glass Fiber Amplifiers Spontaneous Emission Source," U.S. Patent 7423803B1, 2008.
- [7] M. J. F. Digonnet and K. Liu, "Analysis of a 1060-nm Nd:SiO<sub>2</sub> superfluorescent fiber laser," *J. Lightw. Technol.*, vol. 7, no. 7, pp. 1009–1015, Jul. 1989.
- [8] S. V. Chernikov, J. R. Taylor, V. P. Gapontsev, B. E. Bouma, and J. G. Fujimoto, "A 75-nm, 30-mW superfluorescent ytterbium fiber source operating around 1.06  $\mu\text{m}$ ," in *Proc. Conf. Lasers and Electro-Optics (CLEO '97)*, 1997, vol. 11, pp. 83–84.
- [9] R. Paschotta, J. Nilsson, A. C. Tropper, and D. C. Hanna, "Efficient superfluorescent light sources with broad bandwidth," *IEEE Sel. Topics Quantum Electron.*, vol. 3, no. 4, pp. 1097–1099, Aug. 1997.
- [10] J. M. Sousa, M. Melo, L. A. Ferreira, J. R. Salcedo, and M. O. Berendt, "Product design issues relating to rare-earth doped fiber ring lasers and superfluorescent sources," *Proc. SPIE*, vol. 6102, pp. 610223.1–610223.12, 2006.
- [11] A. B. Lobo Ribeiro, I. Trifanov, M. A. R. Melo, M. O. Berendt, R. Romero, and J. R. Salcedo, "Broadband Neodymium-Ytterbium-Silica Doped Amplified Spontaneous Emission Optical Fiber Source by Spectral Filtered Reinjecting Signals," U.S. Patent Pending 12/482670, 2009.
- [12] G. Rego, O. Okhotnikov, E. Dianov, and V. Sulimov, "High-temperature stability of long-period fiber gratings produced using an electric arc," *J. Lightw. Technol.*, vol. 19, no. 10, pp. 1574–1579, Oct. 2001.
- [13] L. Neagu, A. Lobo Ribeiro, J. Salcedo, R. G. Cucu, A. Bradu, L. Ma, J. Bloor, and A. G. Podoleanu, "Frequency shifter based *en-face* OCT system at 1060 nm," in *Proc. Topical Meeting on Optoinformatics of the 5th Int. Optical Congress (Optoinformatics '08)*, St. Petersburg, Russia, 2008, p. 143.
- [14] A. G. Podoleanu and D. A. Jackson, "Combined optical coherence tomography and scanning laser ophthalmoscope," *Electron. Lett.*, vol. 34, no. 11, pp. 1088–1090, 1998.
- [15] R. C. Cucu, A. G. Podoleanu, J. A. Rogers, J. Pedro, and R. B. Rosen, "Combined confocal/*en-face* T-scan-based ultrahigh-resolution optical coherence tomography in vivo retinal imaging," *Opt. Lett.*, vol. 34, no. 11, pp. 1684–1686, 2006.